Published in final edited form as:

Ophthalmol Retina. 2024 January ; 8(1): 42–48. doi:10.1016/j.oret.2023.08.017.

Classification and growth rate of chorioretinal atrophy after voretigene neparvovec-rzyl for RPE65-mediated retinal degeneration

Nikhil Bommakanti, MD[1], **Benjamin K Young, MD, MS**[1], **Robert A Sisk, MD**[2,3,4], **Audina M Berrocal, MD**[5], **Jacque L Duncan, MD**[6], **Benjamin Bakall, MD, PhD**[7], **Marc T Mathias, MD**[8], **Ishrat Ahmed, MD, PhD**[9], **Sarah Chorfi, MD**[9], **Jason Comander, MD, PhD**[9], **Aaron Nagiel, MD, PhD**[10,11], **Cagri G Besirli, MD, PhD**[1]

[1.]Department of Ophthalmology and Visual Sciences, W.K. Kellogg Eye Center, University of Michigan Medical School, Ann Arbor, MI

[2.]Cincinnati Eye Institute, Cincinnati, Ohio.

[3.]University of Cincinnati Department of Ophthalmology, Cincinnati, Ohio.

[4.]Abrahamson Pediatric Eye Institute, Cincinnati Children's Hospital Medical Center, Cincinnati, Ohio.

[5.]Bascom Palmer Eye Institute, University of Miami, Miami, Florida.

[6.]Department of Ophthalmology, University of California, San Francisco, California

[7.]Associated Retina Consultants, Phoenix, AZ

[8.]Department of Ophthalmology, University of Colorado Denver School of Medicine, Aurora, Colorado

[9.]Ocular Genomics Institute, Department of Ophthalmology, Massachusetts Eye and Ear, Harvard Medical School, Boston, Massachusetts

[10.]The Vision Center, Department of Surgery, Children's Hospital Los Angeles, Los Angeles, California.

[11.]Roski Eye Institute, Department of Ophthalmology, Keck School of Medicine, University of Southern California, Los Angeles, California.

Corresponding Author and Address for Reprints: Cagri G. Besirli, MD, PhD, W.K. Kellogg Eye Center, Department of Ophthalmology and Visual Sciences, 1000 Wall Street, Ann Arbor, MI 48105, cbesirli@med.umich.edu.

R.A.S.: Consulting – AGTC, Allergan, EyePoint, Gyroscope, Leica, Orbit Biomedical, REGENXBIO; Travel/accommodation – REGENXBIO.

J.L.D.: Royalties – McGraw-Hill; Payment for development of educational presentations – WebMD; Board Membership – Foundation Fighting Blindness; Consulting – AGTC, Conesight, DTx Pharma, Editas, Eyevensys, Gyroscope, Helios, Nacuity, ProQR Therapeutics, PYC Therapeutics, Relay, SparingVision, Spark Therapeutics, Vedere Bio; Grants – Acucela, AbbVie/Allergan, Biogen, PYC Therapeutics, Foundation Fighting Blindness, Unrestricted Grant to Research to Prevent Blindness to USCF.

B.K.Y.: Grant – Heed Ophthalmic Foundation.

J.C.: Grants – NIH R01 EY031036

A.N.: Grants – Unrestricted grant by Research to Prevent Blindness to the Department of Ophthalmology at the USC Kech School of Medicine, Knights Templar Eye Foundation, Las Madrinas Endowment in Experimental Therapeutics for Ophthalmology, NIH/NEI Career Development Award K08EY030924, Research To Prevent Blindness Career Development Award.

C.G.B.: Grants – The E. Matilda Ziegler Foundation for the Blind, The Retina Society, NIH/NEI R01EY029675.

Abstract

Purpose—Classify the appearance and quantify the growth rate of chorioretinal atrophy in patients who received voretigene neparvovec-rzyl (VN) for *RPE65*-mediated retinal degeneration.

Design—Multicenter retrospective analysis

Subjects—Patients who underwent subretinal VN injection at 5 institutions and demonstrated posterior pole chorioretinal atrophy.

Methods—Ultra-widefield scanning laser ophthalmoscopy or color fundus photos were assessed before and after subretinal VN. Atrophy was defined as regions with at least two of the following: (1) partial or complete retinal pigment epithelial (RPE) depigmentation, (2) round shape, (3) sharp margins, (4) increased visibility of choroidal vessels. Atrophy was qualitatively classified into different subtypes. All atrophy was manually segmented. Linear mixed effects models with random slopes and intercepts were fit using atrophy area and square root of atrophy area.

Main Outcome Measures—Number of eyes with each atrophy pattern, and slopes of linear mixed effects models.

Results—Twenty-seven eyes from 14 patients across 5 centers developed chorioretinal atrophy after subretinal VN. A mean of 5.8 ± 2.7 images per eye obtained over 2.2 ± 0.8 years were reviewed, and atrophy was categorized into *touchdown* (14 eyes), *nummular* (15 eyes), and *perifoveal* (12 eyes) subtypes. Fifteen eyes demonstrated more than one type of atrophy. Thirteen of 14 patients demonstrated bilateral atrophy.

The slopes of the mixed effects models of atrophy area and square root of atrophy area (estimate ± standard error) were 1.7 ± 1.3mm^2/year and 0.6 ± 0.2 mm/year for touchdown atrophy, 5.5 ± 1.3 mm^2/year and 1.2 ± 0.2 mm/year for nummular atrophy, and 16.7 ± 1.8 mm^2/year and 2.3 ± 0.2 mm/year for perifoveal atrophy. The slopes for each type of atrophy were significantly different in the square root of atrophy model, which best fit the data ($p < 0.05$).

Conclusions—Chorioretinal atrophy following subretinal VN for *RPE65*-mediated retinal degeneration developed according to a touchdown, nummular, and/or perifoveal pattern. Perifoveal atrophy grew the most rapidly whereas touchdown atrophy grew the least rapidly. Understanding the causes of these findings, which are present in a minority of patients, merits further investigation.

Précis—Retinal atrophy following voretigene neparvovec-rzyl for *RPE65*-mediated retinal degeneration conformed to different patterns which also grew at different rates. The potential causes of these findings are discussed.

Keywords

Chorioretinal atrophy; voretigene neparvovec-rzyl; Luxturna; growth rate; gene therapy; Leber congenital amaurosis

Introduction

Voretigene neparvovec-rzyl (VN) was approved in December 2017 for the treatment of patients with biallelic *RPE65* mutation-associated retinal degeneration, representing the

first gene therapy approved in the U.S. that targets a disease caused by mutations in a specific gene.[1] VN is a recombinant adeno-associated virus serotype 2 (AAV2) vector which contains complementary DNA for human *RPE65*.[2] The *RPE65* gene encodes the retinoid isomerohydrolase RPE65, which catalyzes the conversion of all-trans-retinyl esters to 11-cis-retinol, a critical step in the retinoid cycle where visual pigments are regenerated after exposure to light.[3,4] Leber congenital amaurosis (LCA) is a heterogeneous group of inherited retinal degenerations associated with mutations in multiple genes, including *RPE65*, which affects an estimated 1 in 33,000 to 81,000 individuals and results in severe visual impairment at birth followed by progressive vision loss.[5] Of note, some cases of *RPE65*-associated retinal degeneration present as early onset retinitis pigmentosa.

We previously reported on the development of perifoveal chorioretinal atrophy after subretinal administration of VN for patients with LCA caused by biallelic *RPE65* mutations,[6] a finding which was not found in the original phase 3 clinical trial.[2] Despite the development of atrophy, these 18 eyes demonstrated no change in visual acuity and maintained improvement in full-field stimulus threshold (FST), likely due to the fovea-sparing nature of the atrophy; however, paracentral scotomata developed in 3 eyes. Similar chorioretinal atrophy after VN has recently been reported elsewhere.[7] No worsening in visual acuity, visual fields, or FST were seen in this series of 13 eyes from 8 patients after a mean of 15.3 months of follow up, although poor baseline visual function may have prevented accurate measurement of functional loss.[7]

In this report, we characterize VN-associated outer retinal degeneration into different subtypes and determine the atrophy growth rates in a larger cohort with greater follow up. The evolution of the three different atrophy patterns may give insight into their causes. This information may become increasingly important as AAV-based gene therapy with VN and other investigational products continues.

Methods

Patient Selection

A retrospective chart review was performed on all patients who received bilateral subretinal VN injection at each of five participating institutions, as described previously.[6] The standard dose of 1.5×10^{11} vg VN in 0.3 mL was directly administered into the subretinal space (i.e. there was no saline “pre-bleb) using foot-pedal-controlled pneumatic pressure provided by the vitrectomy machine and verified with intraoperative optical coherence tomography (OCT), as described in Gange et al.[6] All eyes which demonstrated atrophy (as defined below) involving the perifovea were included in this analysis.

This study was approved by the Institutional Review Boards at the Children’s Hospital Los Angeles, University of Miami, University of Cincinnati, Massachusetts Eye and Ear, and University of Michigan, as well as the University of California San Francisco, where some photographs were taken. This study also complied with the Health Insurance Portability and Accountability Act and adhered to the tenets of the Declaration of Helsinki.

Data and Outcome Measures

Preoperative and all postoperative ultra-widefield scanning laser ophthalmoscopy or color fundus photographs were analyzed. All ultra-widefield scanning laser ophthalmoscopy images were automatically adjusted for area quantification using the included software.[8] Main outcome measures included numbers of eyes belonging to different classifications, as well as rates of change of the linear mixed effects models of atrophy area and square root of atrophy area (i.e., proportional to the effective radius of atrophic lesions) versus time.

Atrophy Definition and Classification

A modified Age-Related Eye Disease Study 2 (AREDS2) definition of atrophy was used.[9] Atrophy was defined as regions which satisfied at least two of the following criteria: (1) partial or complete depigmentation of the retinal pigment epithelium (RPE), (2) round shape, (3) sharp margins, (4) increased visibility of underlying choroidal vessels. Atrophy appearance was reviewed and classified into separate categories based on the most prominent feature.

Image Segmentation

Atrophy and the optic disc, for scale (see below), were manually segmented by two graders using ImageJ version 2.1.0/1.53c (National Institutes of Health, Bethesda, MD, USA).[10] This method of segmentation is adapted from previously validated manual segmentation used in other studies examining color fundus photos for geographic atrophy.[11] The images were classified jointly by the first, second, and senior authors. Segmentations and classifications were reviewed by the primary surgeon for each patient, who had the opportunity to reclassify images for their patients. No images were reclassified.

Growth Rates

Total atrophy area and square root of total atrophy area were calculated for each image. Manual areas of segmentation were converted to millimeters by scaling to an optic disc diameter of 1.8 millimeters, based on the AREDS2 definition,[9] after determining the optic disc diameter by fitting a circle which best accommodated the vertical disc dimension, then calculating its diameter.

Linear mixed effects models with random slopes and intercepts of atrophy area versus time and square root of atrophy area versus time were fit for atrophy characterized as touchdown, nummular, perifoveal, or mixed (see the Results section) in eyes which demonstrated these types of atrophy. The use of linear mixed effects models also addressed possible inter-eye correlation. Growth rates were measured using the slopes of the model. Data analysis was performed with Python version 3.8.12 using the numpy, pandas, skimage, and roifile packages, and statistical analysis was performed with R version 4.1.3 using the lme4, lmerTest, and interactions packages.

Results

Twenty-seven eyes from 14 patients developed chorioretinal atrophy after subretinal administration of VN (see Figure 1, available at https://www.ophthalmologyretina.org/, for

an OCT image confirming the presence of chorioretinal atrophy). A total of 187 eyes had been treated by the time of the last follow up, resulting in a prevalence of 14.4%. Patients were followed for (mean ± standard deviation) 2.2 ± 0.8 (range: 0.8 to 3.9) years and received 5.8 ± 2.7 (range: 2 to 11) fundus photographs. Ultra-widefield scanning laser ophthalmoscopy images were used for all but 2 eyes, in which widefield imaging was used. Mean age was 13.4 ± 5.8 years (range: 5 to 26 years), and 9 patients (64.3%) were male. The mean spherical equivalent was −4.0 ± 4.1 diopters (range: −11.50 to +2.00). Demographic and ophthalmic data for all eyes and separated by atrophy subtype are shown in Table 1.

Atrophy classification

Several patterns of atrophy were observed (Figure 2). Atrophy subtypes included atrophy at the injection site (*touchdown*; 14 [51.9%] eyes; Figure 2A); nummular areas of atrophy predominantly involving the periphery (*nummular*; 15 [55.6%] eyes; Figure 2B); and atrophy predominantly in the perifoveal region (*perifoveal*; 12 [44.4%] eyes; Figure 2C). Five (18.5%) eyes demonstrated atrophy with confluent patterns of nummular and perifoveal atrophy where the two could not be differentiated (Figure 2D). Twelve eyes demonstrated 1 type of atrophy, 10 eyes demonstrated 2 types of atrophy, and 5 eyes demonstrated all 3 types of atrophy. All 27 eyes demonstrated atrophy in the macula and 20 eyes demonstrated atrophy in the periphery.

Bilaterality and fellow eye correspondence

Thirteen of 14 patients demonstrated bilateral atrophy (the 14th patient demonstrated perifoveal and touchdown atrophy in one eye and only touchdown atrophy in the fellow eye, which was excluded). Ten of the 14 eyes with touchdown site atrophy, 14 of the 15 eyes with nummular atrophy, and 8 of the 12 eyes with perifoveal atrophy were fellow eyes from the same patient.

Growth rate and model fit

The atrophy growth rate by area and by square root of area (mean ± standard error) for the 25 of 27 eyes (14 of 14 eyes with touchdown atrophy, 13 of 15 eyes with nummular atrophy, 12 of 12 eyes with perifoveal atrophy, and 5 of 5 eyes with mixed atrophy) with more than two follow up images were measured. The touchdown atrophy growth rates were 1.7 ± 1.3 mm^2/year and 0.6 ± 0.2 mm/year, the nummular atrophy growth rates were 5.5 ± 1.3 mm^2/year and 1.2 ± 0.2 mm/year, the perifoveal atrophy growth rates were 16.7 ± 1.8 mm^2/year and 2.3 ± 0.2 mm/year, and the mixed atrophy growth rates were 25.3 ± 2.2 mm^2/year and 2.8 ± 0.3 mm/year (Figure 3, as well as Figures 4 and 5, available at https://www.ophthalmologyretina.org/). The data were fit better with the square root of atrophy model (Akaike information criterion 969.8 vs. 2115.8). Growth rates of touchdown, nummular, and perifoveal atrophy were significantly different ($p < 0.05$) in the square root model.

Discussion

This study describes the characteristics and growth rate of VN-associated chorioretinal atrophy over a mean of 2.2 years in 27 eyes from 14 patients who received VN for biallelic

RPE65-associated retinal degeneration. Demographic and ophthalmic data, including sex, age, spherical equivalent refraction, and baseline FST, for patients who did and did not develop VN-associated chorioretinal atrophy have been compared in a separate report.[12] Table 1 presents these data for all eyes with chorioretinal atrophy and for eyes with each atrophy subtype.

Different subtypes, each with distinct rates of growth, were identified. Perifoveal atrophy had the most rapid growth rate and touchdown site atrophy had the slowest growth rate; nummular atrophy demonstrated an intermediate growth rate. The indeterminate mixed pattern demonstrated characteristics of both nummular and perifoveal atrophy in both appearance and growth rate. This group represented atrophy with confluent patterns of nummular and perifoveal atrophy where the two could not be differentiated, which likely explains the higher growth rate.

For comparison, even the slowest growth rate of 0.5 ± 0.3 mm/year in the square root transformed model of touchdown atrophy was greater than that of multifocal geographic atrophy in age-related macular degeneration, which was determined to be 0.199 ± 0.012 mm/year in a meta-analysis.[13] These differences in growth rates suggest different underlying mechanisms, or differing relative contributions from multiple mechanisms, as discussed below.

Bilateral atrophy occurred in 13 of 14 patients in this series; furthermore, the same subtype of atrophy tended to occur in both eyes. This effect was observed across surgeries performed at different institutions on different dates by different surgeons, suggesting an inherent predisposition in certain patients. Chorioretinal atrophy inside and outside the region of the bleb(s) were also observed in another study, further suggesting against a surgeon-specific factor.[7]

All eyes in this series demonstrated outer retinal degeneration within the macula. Other diseases with macular atrophy, such as age-related macular degeneration or Stargardt disease, have rates of growth which correlate best with effective radius, which is linearly proportional to the square root of atrophy.[13–15] Here, the square root of atrophy model also better fit the data, which may suggest a similar fundamental mechanism to what occurs in more common forms of macular degeneration.

A limitation of this paper is the subjective nature of the classifications, which were based on the most prominent feature and did not prioritize shape or location. There may be a spectrum of findings, as suggested by the mixed category. Of note, perifoveal atrophy was defined previously.[6] The small sample size of this study may limit the ability to reliably categorize the different patterns of chorioretinal atrophy and the generalizability of these findings. Other limitations of this study include its retrospective design, limited longitudinal follow up, and manual segmentation of atrophy, although the manual segmentation technique has been previously described.[14] Scanning laser ophthalmoscopy may not be the optimal technique to quantify atrophy; for example, OCT has been used to quantify other types of chorioretinal atrophy.[16,17] Near-infrared imaging may have been superior. Autofluorescence images may be considered, however these patients tend to have limited autofluorescence

signal. Ultra-widefield OCT and autofluorescence images of the peripheral atrophy were not available for segmentation in all patients in the current study. Furthermore, many of the treated patients have poor fixation which can result in poor quality OCT imaging. One advantage of the current study is the images were scaled to ensure peripheral lesions were comparable to macular lesions for area quantification.[8] The use of widefield color photos for two eyes may have led to an underestimated rate of nummular lesions (i.e., if these eyes had nummular lesions, the incidence would be 63.0% rather than 55.6%). Finally, this mathematical analysis does not directly reveal the mechanism(s) underlying this recently observed phenomenon.

Due to the inaccessibility of the treated tissues in patients treated with VN, it may be difficult to directly determine the cause of each type of atrophy pattern observed. Possible mechanisms include mechanical factors such as tissue indentation from the injection cannula, shear forces from fluid propagation, or trauma from the transient retinal detachment; vector toxicity or target overproduction; and inflammation. G-protein activation by mislocalized opsin has been hypothesized as well.[18,19] Given the distinct growth rates, the atrophy subtypes may be driven by different combinations of multiple mechanisms. The touchdown atrophy may be more influenced by surgical factors, whereas the nummular and perifoveal subtypes may be more driven by toxicity or inflammation. Reallocation of cellular machinery toward production of the vector target, potentially to the detriment of critical cellular functions, may also lead to atrophy in cells that are already compromised secondary to underlying disease. The overlap of atrophy phenotypes may indicate there is a spectrum of atrophic changes that are modulated by an additional factor, such as distance from the fovea.

Animal data allows for more specific hypotheses about toxicity and, in mice, AAV vectors with ubiquitous promoter or promoters that express in the RPE cause a dose-dependent atrophy.[20] VN uses a hybrid chicken β-actin promoter with a cytomegalovirus enhancer.[2] Long term follow-up of human AAV gene therapy programs with photoreceptor-specific promoters would be instructive. Subclinical subretinal inflammation has been seen in mice and nonhuman primates.[20,21] This tends to be dose dependent, whereas all patients in this report were treated with the same concentration of VN. An assessment of dose dependency may be possible by analyzing outcomes of VN clinical trial patients treated with lower doses. Finally, this posttreatment atrophy may occur due to an acceleration of disease, which may result in atrophy developing in areas which were already most affected by disease, although this was not specifically evaluated.

Perifoveal atrophy was required for inclusion in this study, therefore the 14.4% prevalence determined in this study may underestimate the prevalence of any chorioretinal atrophy after VN. Notably, however, this value is similar to the rate of 12.6% (13/103) reported by the PERCEIVE study.[22] For context, due to the persistence of beneficial treatment effects even in patients experiencing atrophy (see Introduction), and the poor natural history of the underlying disease, treatment with VN continues in all the treatment centers which contributed patients to this report. However, these patients should continue to be followed to evaluate the extent of atrophy and its potential effect on visual function. While a preliminary

report suggests that the atrophy appears in the minority of patients,[22] it would also be helpful to analyze the incidence rate more formally.

Conclusion

Chorioretinal atrophy following subretinal administration of VN for *RPE65*-mediated retinal degeneration developed according to touchdown site, nummular, and/or perifoveal patterns. Perifoveal atrophy grew the most rapidly whereas touchdown site atrophy grew the least rapidly. Atrophy growth was more strongly correlated with square root of atrophy area rather than atrophy area, as observed in other causes of macular atrophy such as dry age-related macular degeneration. These findings demonstrate the need for close observation in studies involving other gene therapies using similar vectors.

Supplementary Material

Refer to Web version on PubMed Central for supplementary material.

Financial Support:

NB: None.

BKY: Heed Ophthalmic Foundation

RAS: None.

AMB: None.

JLD: This research was supported, in part, by the UCSF Vision Core shared resource of the NIH/NEI P30 EY002162, by the Foundation Fighting Blindness, and by the Research to Prevent Blindness Unrestricted Grant to UCSF.

BB: None.

MTM: None.

IA: None.

SC: None.

JC: None.

AN: Unrestricted grant to the Department of Ophthalmology at the USC Keck School of Medicine from Research to Prevent Blindness, an endowment from the Knights Templar Eye Foundation, the Las Madrinas Endowment in Experimental Therapeutics for Ophthalmology, NIH/NEI Career Development Award K08EY030924, and a Research To Prevent Blindness Career Development Award. These funding organizations had no role in the design or conduct of this research.

CGB: Research awards from The E. Matilda Ziegler Foundation for the Blind, The Retina Society, NIH/NEI R01EY029675. Employee, Janssen Research and Development. These funding organizations had no role in the design or conduct of this research.

Abbreviations:

VN	Voretigene neparvovec
RPE	retinal pigment epithelium

AAV2	adeno-associated virus serotype 2
LCA	Leber congenital amaurosis
FST	full-field stimulus threshold
AREDS2	Age-Related Eye Disease Study 2

References

1. Food and Drug Administration. FDA 2019. Available at: https://www.fda.gov/vaccines-blood-biologics/cellular-gene-therapy-products/luxturna [Accessed December 29, 2021].
2. Russell S, Bennett J, Wellman JA, et al. Efficacy and safety of voretigene neparvovec (AAV2-hRPE65v2) in patients with RPE65 -mediated inherited retinal dystrophy: a randomised, controlled, open-label, phase 3 trial. The Lancet 2017;390:849–860.
3. Moiseyev G, Chen Y, Takahashi Y, et al. RPE65 is the isomerohydrolase in the retinoid visual cycle. Proc Natl Acad Sci 2005;102:12413–12418.
4. Redmond TM, Poliakov E, Yu S, et al. Mutation of key residues of RPE65 abolishes its enzymatic role as isomerohydrolase in the visual cycle. Proc Natl Acad Sci 2005;102:13658–13663.
5. Kumaran N, Moore AT, Weleber RG, Michaelides M. Leber congenital amaurosis/early-onset severe retinal dystrophy: clinical features, molecular genetics and therapeutic interventions. Br J Ophthalmol 2017;101:1147–1154. [PubMed: 28689169]
6. Gange WS, Sisk RA, Besirli CG, et al. Perifoveal Chorioretinal Atrophy after Subretinal Voretigene Neparvovec-rzyl for RPE65-Mediated Leber Congenital Amaurosis. Ophthalmol Retina 2022;6:58–64. [PubMed: 33838313]
7. Reichel FF, Seitz I, Wozar F, et al. Development of retinal atrophy after subretinal gene therapy with voretigene neparvovec. Br J Ophthalmol 2022:bjophthalmol-2021–321023.
8. Croft DE, van Hemert J, Wykoff CC, et al. Precise Montaging and Metric Quantification of Retinal Surface Area From Ultra-Widefield Fundus Photography and Fluorescein Angiography. Ophthalmic Surg Lasers Imaging Retina 2014;45:312–317. [PubMed: 25037013]
9. Danis RP, Domalpally A, Chew EY, et al. Methods and Reproducibility of Grading Optimized Digital Color Fundus Photographs in the Age-Related Eye Disease Study 2 (AREDS2 Report Number 2). Invest Ophthalmol Vis Sci 2013;54:4548–4554. [PubMed: 23620429]
10. Schindelin J, Arganda-Carreras I, Frise E, et al. Fiji: an open-source platform for biological-image analysis. Nat Methods 2012;9:676–682. [PubMed: 22743772]
11. Shen LL, Sun M, Ahluwalia A, et al. Relationship of Topographic Distribution of Geographic Atrophy to Visual Acuity in Nonexudative Age-Related Macular Degeneration. Ophthalmol Retina 2021;5:761–774. [PubMed: 33212271]
12. Stingl K, Stingl K, Schwartz H, et al. Full-field scotopic threshold improvement following voretigene neparvovec-rzyl treatment correlates with chorioretinal atrophy. Ophthalmology 2023;0. Available at: https://www.aaojournal.org/article/S0161-6420(23)00126-4/fulltext [Accessed February 26, 2023].
13. Shen LL, Sun M, Grossetta Nardini HK, Del Priore LV. Progression of Unifocal versus Multifocal Geographic Atrophy in Age-Related Macular Degeneration. Ophthalmol Retina 2020;4:899–910. [PubMed: 32423772]
14. Shen LL, Sun M, Ahluwalia A, et al. Geographic Atrophy Growth Is Strongly Related to Lesion Perimeter. Ophthalmol Retina 2020:S2468653020304826.
15. Shen LL, Sun M, Grossetta Nardini HK, Del Priore LV. Natural History of Autosomal Recessive Stargardt Disease in Untreated Eyes. Ophthalmology 2019;126:1288–1296. [PubMed: 31227323]
16. Holz FG, Sadda SR, Staurenghi G, et al. Imaging Protocols in Clinical Studies in Advanced Age-Related Macular Degeneration: Recommendations from Classification of Atrophy Consensus Meetings. Ophthalmology 2017;124:464–478. [PubMed: 28109563]

17. Sadda SR, Guymer R, Holz FG, et al. Consensus Definition for Atrophy Associated with Age-Related Macular Degeneration on OCT: Classification of Atrophy Report 3. Ophthalmology 2018;125:537–548. [PubMed: 29103793]

18. Townes-Anderson E. Increased levels of gene therapy may not be beneficial in retinal disease. Proc Natl Acad Sci U S A 2013;110:E1705.

19. Cideciyan AV, Jacobson SG, Beltran WA, et al. Reply to Townes-Anderson: RPE65 gene therapy does not alter the natural history of retinal degeneration. Proc Natl Acad Sci U S A 2013;110:E1706.

20. Xiong W, Wu DM, Xue Y, et al. AAV cis-regulatory sequences are correlated with ocular toxicity. Proc Natl Acad Sci 2019;116:5785–5794. [PubMed: 30833387]

21. Rodríguez-Bocanegra E, Wozar F, Seitz IP, et al. Longitudinal Evaluation of Hyper-Reflective Foci in the Retina Following Subretinal Delivery of Adeno-Associated Virus in Non-Human Primates. Transl Vis Sci Technol 2021;10:15.

22. Fischer MD, Maier R, Suhner A, et al. PERCEIVE study report: Real-world safety and effectiveness of voretigene neparvovec. Invest Ophthalmol Vis Sci 2022;63:451.

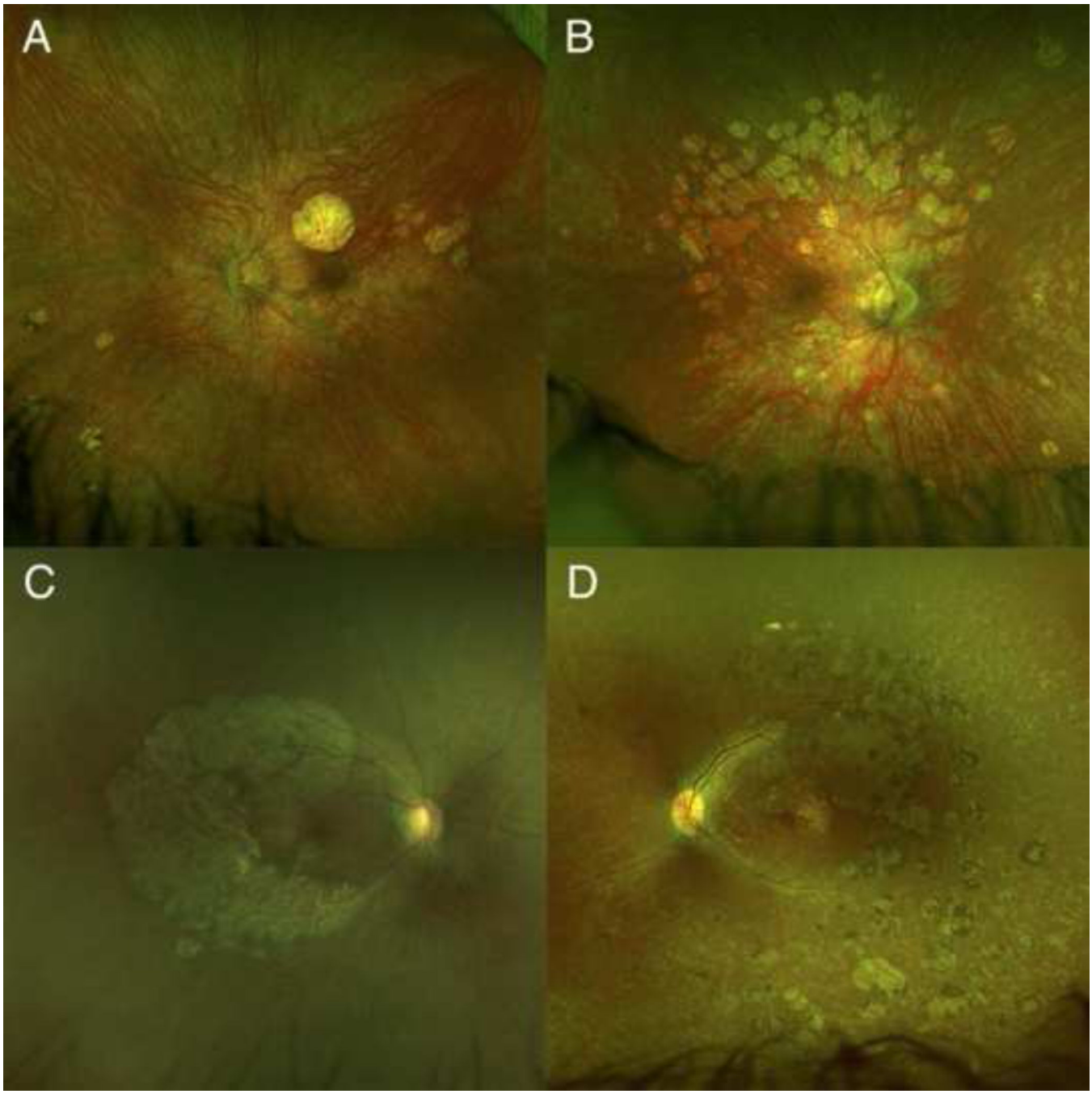

Figure 2.
Examples of eyes demonstrating touchdown (Panel A), nummular (Panel B), perifoveal (Panel C), and mixed (Panel D) atrophy.

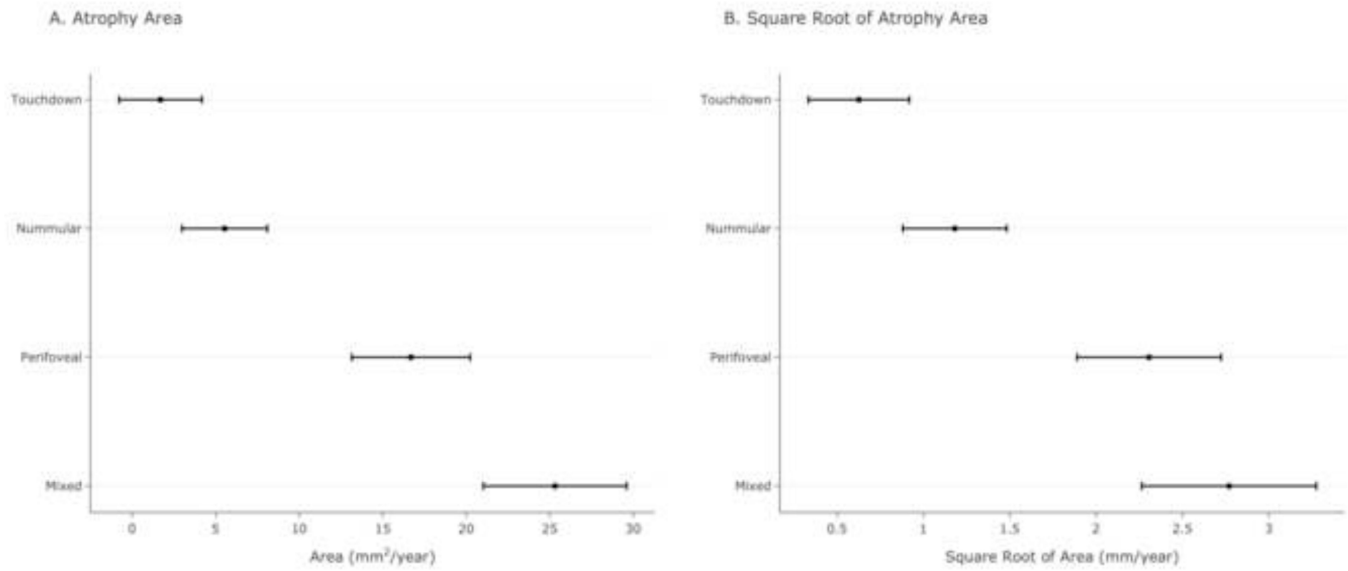

Figure 3.

Atrophy growth rates. Slopes and standard errors of the linear mixed effects models for each type of atrophy using atrophy area (A) and square root of atrophy area (B).

Table 1.

Baseline Characteristics Separated by Atrophy Subtype. Male sex and length of follow up are summarized at the patient level. FST is provided for those eyes which underwent this assessment at the baseline visit (18, 9, 12, 4, and 4 eyes for all eyes and for the touchdown, nummular, perifoveal, and mixed groups, respectively). Fifteen eyes demonstrated more than one type of atrophy.

	All (27 eyes, 14 patients)		**Touchdown (14 eyes, 9 patients)**		**Nummular (15 eyes, 8 patients)**		**Perifoveal (12 eyes, 9 patients)**		**Mixed (5 eyes, 3 patients)**	
	Mean or N	**SD or %**	**Mean or N**	**SD or %**	**Mean or N**	**SD or %**	**Mean or N**	**SD or %**	**Mean or N**	**SD or %**
Age, mean years (SD)	13.4	5.8	13.4	6.6	14.3	6.9	12.2	6.6	12	3.4
Male, N (%)	9	64.3	4	44.4	4	50	5	62.5	2	66.7
Follow up, years (SD)	2.7	1.6	3.6	1.6	3.2	2	2.7	1.6	2.5	0.3
Spherical equivalent, mean D (SD)	−4	4.1	−3.9	3.9	−4.8	4.4	−3.1	3.4	−4.4	4.6
Baseline visual acuity, mean logMAR (SD)	0.8	0.4	0.7	0.3	0.7*	0.3	1*	0.4	0.8	0.3
Baseline FST, mean $\log_{10}(cd.s/m^2)$ (SD)	−1.9	0.8	−2.3	0.8	−2.1	0.8	−2.4	0.5	−1.2	0.4

*P < 0.05 by analysis of variance with post-hoc Tukey HSD testing between the touchdown, nummular, perifoveal, and mixed groups. Decimals are rounded to the nearest tenth.

SD: standard deviation, N: number, D: diopters, logMAR: logarithm of the minimum angle of resolution, FST: full-field stimulus threshold.